Eur. Phys. J. D **40**, 305–311 (2006)
DOI: 10.1140/epjd/e2006-00148-5

THE EUROPEAN PHYSICAL JOURNAL D

Generation of attosecond pulses in molecular nitrogen

H. Wabnitz[1,a], Y. Mairesse[1,b], L.J. Frasinski[2], M. Stankiewicz[2,4], W. Boutu[1], P. Breger[1], P. Johnsson[3], H. Merdji[1], P. Monchicourt[1], P. Salières[1], K. Varjú[3], M. Vitteau[1], and B. Carré[1]

[1] CEA/DSM/DRECAM/SPAM, bâtiment 522, Centre d'Études de Saclay, 91191 Gif-sur-Yvette, France
[2] J.J. Thomson Physical Laboratory, The University of Reading, Whiteknights, Reading RG6 6AF, UK
[3] Department of Physics, Lund University, P.O. Box 118, 22100 Lund, Sweden
[4] Institute of Physics, Jagellonian University, ul. Reymonta 4, 30-059 Krakow, Poland

Received 13 December 2005 / Received in final form 16 March 2006
Published online 28 June 2006 –

Abstract. We have generated attosecond pulse trains in an ensemble of randomly aligned nitrogen molecules. Measurements of the high-order harmonic relative phases and amplitudes allow us to reconstruct the temporal profile of the attosecond pulses. We show that in the considered spectral range, the latter is very similar to the pulse train generated in argon under the same conditions. We discuss the possible influence of the molecular structure in the generation process, and how it can induce subtle differences on the relative phases.

PACS. 42.65.Ky Frequency conversion; harmonic generation, including higher-order harmonic generation – 42.65.Re Ultrafast processes; optical pulse generation and pulse compression – 33.80.Wz Other multiphoton processes

1 Introduction

High harmonic generation (HHG) in the extreme ultraviolet range has drawn much of attention after its first manifestation almost two decades ago [1,2]. Recent experimental breakthroughs have triggered new interests for this source. First, the production of attosecond pulses in atomic gases by superposing several harmonics was achieved. The production of isolated [3,4] as well as trains of attosecond pulses (APT) [5–7] has been experimentally demonstrated and both have already lead to first applications with attosecond time resolution [8,9]. Furthermore, detailed characterisation of the APT production in atoms has provided a much more profound insight in the underlying electron dynamics [10]. Very recently, it was shown that a thorough characterisation of HHG from aligned molecules could provide a tomographic imaging of the highest occupied molecular orbital [11]. Whereas detailed studies have been performed for the production in atoms, the production of APTs in molecules has not been investigated so far. We will therefore present the first characterisation of an APT generated in randomly aligned N_2 molecules using the RABITT technique (Reconstruction of Attosecond Beating by Interference of Two-Photon Transition) [5,12].

We first give the experimental details and present the set-up in Section 2. In Section 3 we show experimental results for APTs generated in N_2 and compare them to those of an atomic medium (argon). We then discuss the similarities and differences between the two media in the light of the generating process. In the last section (Sect. 4) we discuss further potential consequences on tomographic imaging techniques and give perspectives.

2 Experimental set-up and method

The experimental set-up at the LUCA laser facility is shown in Figure 1. LUCA delivers 50 fs infrared (IR) pulses at 800 nm with a repetition rate of 20 Hz and an energy up to 60 mJ. Shortly after passing a lens ($f = 1$ m), we separate the incoming IR pulse by a beam-splitter (BS) into two parts. The main fraction of energy (75%) (upper path in Fig. 1) generates harmonics in a pulsed gas jet of N_2-molecules (backing pressure = 1.8 bar) positioned closely behind the laser focus (intensity $\sim 1\times10^{14}$ W/cm^2). By focusing the laser before the generating gas jet we ensure the selection of the short quantum path [13–15]. Further downstream a combination of two IR anti-reflective coated SiO_2-plates serves two goals. Firstly it separates the harmonic radiation which is mainly reflected (and absorbed) from the generating laser beam which is mainly

[a] *Present address:* HASYLAB at DESY, Notkestr. 85, 22603 Hamburg, Germany. e-mail: `hubertus.wabnitz@desy.de`
[b] *Present address:* NRC Canada, Steacie Institute for Molecular Sciences, 100 Sussex Drive, Ottawa, Ontario K1A OR6, Canada.

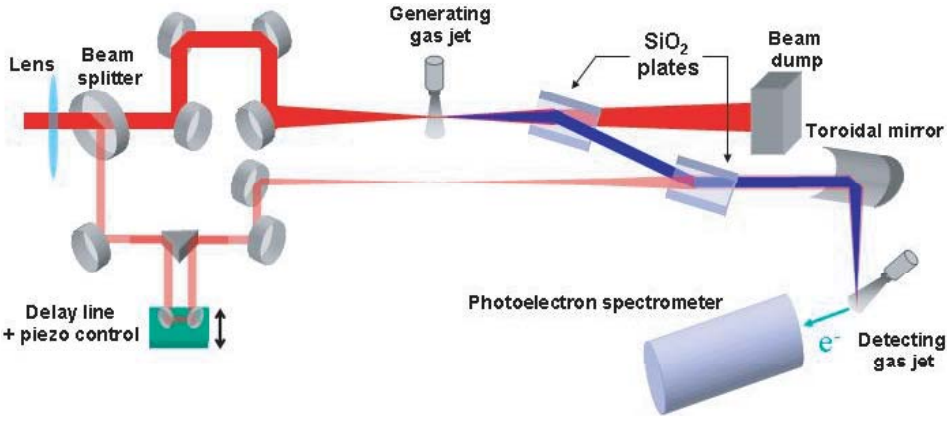

Fig. 1. (Color online) Principal sketch of the experimental set-up. The initial IR laser beam splits into pump and probe branch. The nonlinear interaction of the IR laser in the pump branch with the N_2 molecular jet drives the harmonics production. The harmonics are reflected and refocused into the interaction volume of a MBES, where they produce photo ionisation in argon. Temporal overlap of harmonic pulse and IR probe leads to the appearance of sidebands in the photoelectron energy spectrum.

transmitted. At 10° grazing incidence we have measured an overall reflectivity of the two plates of 1.8% at 800 nm and 30–40% for the 13rd to 21st harmonic. Note that in fact the plates were manufactured for minimum IR reflection at 20°. We decided to use them under 10° in order to increase the harmonic reflectivity and still maintain a suppression of most of the IR pulse energy. We will explain in the next section, why we need a low IR energy in the generating branch. Secondly we use the second SiO_2-plate to recombine the harmonics with the weaker part (25%) of the initial IR pulse, the IR probe beam. In the probe branch after the BS, the beam passes an optical delay line equipped with a piezo electric translation, before it enters the vacuum chamber collinearly to the generating IR beam, with a lateral separation of 40 mm. The separation allows us to pass the probe beam well outside the generating medium and ensure it does not perturb the generation. After traversing the second SiO_2-plate the probe is combined with the harmonics. Further downstream both beams are refocused by a broadband Pt coated toroidal mirror ($f = 70$ cm) under 3° grazing incidence into a gas jet (argon) in the source volume of a magnetic bottle electron spectrometer (MBES) [16].

The resulting photo electron spectra show main lines separated by twice the IR photon energy due to single-photon ionisation by harmonics above the first ionisation limit of argon (15.76 eV). When the dressing IR temporally overlaps with the harmonics, additional absorption (or emission) of IR photons is feasible and sidebands appear in between the harmonic lines. As we use the RABITT technique [5,12] to characterise the APT, we have reduced the intensity of the dressing beam ($\sim 4 \times 10^{11}$ W/cm^2) in such a way that the energy exchange between the ionising electron and the IR field is restricted to one IR photon. Therefore only first-order sidebands are created[1]. By changing the delay between the IR probe and the APT, the intensity of the sidebands oscillates with a periodicity of $T_0/2$, where T_0 is the period of the fundamental IR field [17]. From this oscillation the difference $\varphi(\omega_{q+2}) - \varphi(\omega_q)$ of the neighbouring harmonics q (centred at the frequency $\omega_q = q\omega_0$) and $q + 2$ can be determined. In combination with the measured spectral amplitudes A_q of the harmonics one can now reconstruct the temporal profile $I(t)$ of the harmonic emission:

$$I(t) = \left| \sum_q A_q \exp[-i\omega_q t + i\varphi(\omega_q)] \right|^2 . \quad (1)$$

As mentioned above a small fraction of the generating IR beam passes the combination of the two SiO_2 plates. This residual beam can interfere with the probe IR beam in the interaction region of the MBES. Such optical interference results in an additional modulation of the sidebands with a periodicity of T_0 as the delay varies. This effect does not disturb the RABITT measurement due to its different periodicity. At the same time it allows us to determine the absolute timing of the harmonic emission with respect to IR electric field [18].

3 Experimental results

3.1 Measurements in molecular nitrogen and argon

Our interest lies in the APT generation in N_2 and the specific features due to its molecular structure. Therefore we compare the experimental results for N_2 with an atomic system. In this case we have chosen argon, because the ionisation potential and the intensity-dependent ionisation probability are very similar [19] to those of N_2 ($I_p = 15.58$ eV). So we performed two series of measurements keeping exactly the same experimental conditions, changing only the generating gas from N_2 to argon, thereby making sure that also phase matching in the two media is similar and propagation effects are negligible. For

[1] This was independently confirmed by the absence of higher order sideband frequencies in the Fast Fourier Transform (FFT) spectrum.

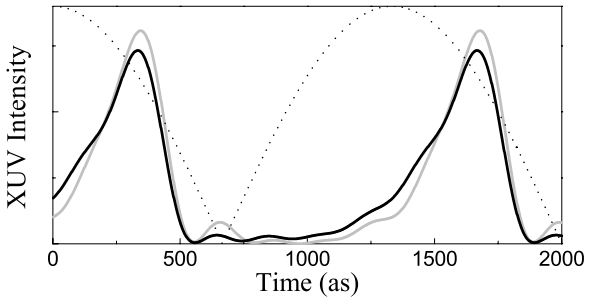

Fig. 2. Reconstructed temporal profiles of attosecond pulses generated in N_2 (black line) and in argon (grey line). The dashed line shows the absolute value of the electric field of the generating IR laser.

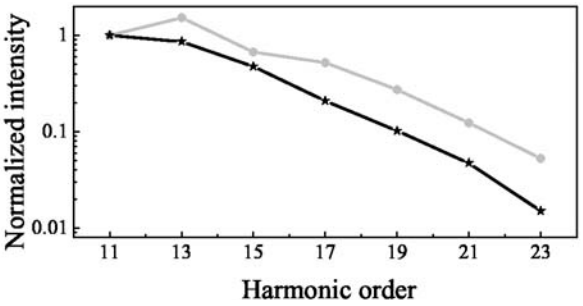

Fig. 3. Normalised harmonic intensities for generation in N_2 (black) and argon (grey).

the analysis of the harmonic emission we have chosen a group of seven harmonics (11th–23rd). The reconstructed temporal profiles of the generated attosecond pulses are shown in Figure 2. The profile obtained in N_2 (black line) is very similar to the one of argon (grey line). Its duration of ∼300 as (FWHM) is slightly longer than for argon (∼280 as). The timing of the two APTs with respect to the IR laser is nearly identical, as can be seen by a comparison to the absolute value of the IR electric field (dotted line) in Figure 2. We would like to note, that we found an additional delay of 300 as compared to the results in [6]. This shift in our set-up is probably due to the dephasing of the IR field with respect to the harmonics during the reflection on the SiO_2-plates. This effect does not affect the comparison of harmonics from N_2 and argon.

The harmonic intensities for N_2 and argon are compared in Figure 3. As a function of harmonic order both curves show a smooth monotonic decrease of intensity without any extrema. The intensity of N_2 (black line) decreases faster, which is in accordance with earlier results [20].

In Figure 4 we compare the harmonic emission times $t_e = \partial\varphi/\partial\omega$, i.e. the group delays. In the RABITT method, the measurement of the phase of the sideband oscillation [5,12] as the delay varies provides the phase difference between two consecutive harmonics $\varphi(\omega_{q+2}) - \varphi(\omega_q) \approx 2\omega_0 t_e(\omega_{q+1})$. We measure this quantity by Fast Fourier Transforming the sideband oscillation and averaging the phase around the frequency of the oscillation in the Fourier domain. Please note, that even for weak

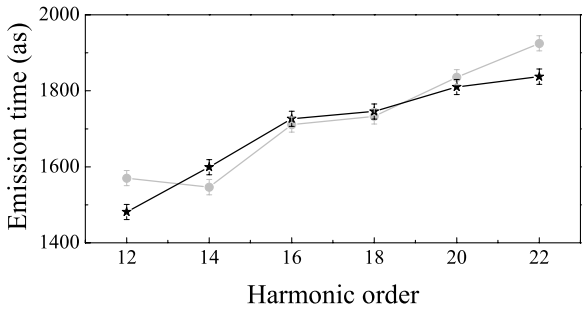

Fig. 4. Harmonic emission times for generation in N_2 (black) and argon (grey). Please note that it is inherent to the RABITT method that emission times are computed at even orders, for further information see text.

sideband intensities the phase of the sideband oscillation is measured with good precision, because the Fourier analysis allows easily to extract the oscillatory from the continuous part. The standard deviation provides the uncertainty on the sideband phase, and therefore on the emission time. An additional uncertainty is due to the measurement of the temporal reference. It is evaluated by the same method, and corresponds to a constant temporal shift of all harmonics.

The emission times of high harmonics generated in N_2 increase approximately linearly with the order, which is characteristic of a linear chirp of the attosecond pulses. This atto chirp can be quantified by measuring the slope of a linear fit of the emission times, and determining the time difference Δt_e between emission of two consecutive harmonics [6]. One obtains for these generating conditions $\Delta t_e^{N_2} = 70 \pm 10$ as. This positive atto chirp of harmonic emission is characteristic of the macroscopic selection of the short quantum path [13,21,22].

The emission times in N_2 can be compared to the ones measured in argon under the same conditions[2]. The atto chirp is in that case $\Delta t_e^{Ar} = 76 \pm 10$ as, which is very close to the value obtained in N_2. On the whole, the harmonic emission times are similar for both generation media. Previous studies in argon have shown that the atto chirp is due to the details of the electron dynamics in the continuum during the generation process. The similarity between the two sets of measurements presented here therefore indicates that these dynamics are very similar in Ar and N_2. In the following, we discuss the details of this generation mechanism and its influence on the harmonic emission times.

3.2 Discussion

The harmonic emission times are determined by the dynamics of the electrons in the generation process. In this section, we present the generation mechanism and discuss

[2] In [6], it was shown that the chirp depends strongly on the laser intensity. In the low ionisation regime, the laser intensity can thus be determined from the chirp value in argon, which yields in our case $\sim 1 \times 10^{14}$ W/cm^2, as mentioned before.

the influence of the generating medium (atomic or molecular).

The mechanism of HHG is well described by a semiclassical three-step-model [23,24]: in the first step, part of the fundamental electron wave function passes to the continuum by tunnelling ionisation. Next this freed electron wave packet (EWP) propagates in the continuum under the influence of the strong electric field of the laser, before it finally, in the third step, recombines with the remaining part of the initial wave function, emitting an XUV photon. The emission time of this photon as well as its energy, are determined by the trajectory of the electron in the continuum and by the ionization potential of the generating medium.

In the three-step-model it is assumed that the laser electric field is so strong that the influence of the Coulomb potential of the remaining ion on the continuum dynamics of the EWP can be neglected. This is one of the assumptions of the so called Strong Field Approximation (SFA) [25]. Therefore, we would expect no strong difference between argon and N_2 because of this. However, it is well-known that the SFA is valid for harmonics in the plateau region, but fails to describe properly low harmonics that are just above the ionisation potential [25]. The low energy of the corresponding EWP makes it more sensitive to the atomic — or molecular — potential. In fact on the experimental results, we observe that the emission time in N_2 deviates significantly from that in argon for harmonic 12, which is just above the ionization potential. This slight but reproducible difference between Ar and N_2 could result from the influence of the Coulomb potentials on the continuum dynamics of the EWPs leading to the emission of the 11th/13th harmonic and could thus be a signature of the molecular structure. This would be an indication that the SFA is only fully valid for sufficiently high harmonic orders, in our case $\geq$15th.

The nature of the generating medium does not only influence the Coulomb potential, but also the electronic structure of the fundamental state. This structure should play an important role in the recombination process. It is known from experiments in aligned molecules [11,26] and theory [27,28] that two-centre molecules exhibit a specific interference pattern. For N_2 the authors of [11] have found a minimum in the harmonic amplitude at the 25th order when the molecular axis was aligned parallel to the laser polarisation.

In reference [26] a minimum was reported for CO_2 at the 23rd order when the angle between molecular axis and laser polarisation is 30°. In another experiment, the minimum was also found but at the 33rd order at the same angle [29]. Lein et al. [27] have predicted and explained this behaviour by the intuitive picture of a two-centre interference: the nuclei of the diatomic molecule are regarded as two point emitters. They are hit coherently by the same electron wave, but with a phase difference that depends on the orientation of the molecular axis with respect to the propagation direction of the electron. The existence of two sources leads to interference effects. Extrema of the emission occur for

$$r_0 \cos(\theta) = \frac{n}{2}\lambda_e \qquad n = 0, 1, 2, ... \tag{2}$$

where r_0 is the internuclear distance. Odd orders of n correspond to minima and even to maxima, when the ground state orbital is symmetric, for example $N_2\, 3\sigma_g$. For an antisymmetric orbital (e.g. $O_2\, 2\pi_g$), the situation is reversed and odd orders correspond to maxima and even to minima. Here the de Broglie wavelength of the electron under the influence of the potential is simply $\lambda_e = h/\sqrt{2m_eE}$, where E is the corresponding harmonic energy. The position of the first extremum on the harmonic spectrum is given by $E = h^2/8m_er_0^2\cos^2\theta$.

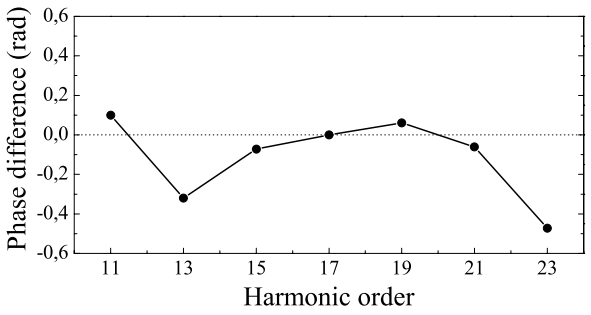

Fig. 5. Difference of harmonic phases generated in N_2 and in argon.

As usual when interference occurs, one would expect a π-jump in the phase. The simulations performed in H_2 [27] indeed show that the minimum in harmonic yield is accompanied by a change in the harmonic phase of about one π-radian. The authors further explain this behaviour with a change of the location in the molecule, from which the leading portion of radiation is emitted. We want to recall that all calculations in [27] were done for H_2^+ and H_2. It is not a priori clear that they hold in detail also for N_2. Nevertheless we feel that a discussion of our experimental results within the above picture might be interesting, also because our measurements are the first of harmonic phases in molecules.

The first minimum in the harmonic emission for N_2 aligned with the laser polarisation was found in [11] to be the 25th harmonic. Below this order, the harmonic relative phases are expected to be determined by the electron dynamics in the continuum. This can be compared with the difference of the relative phases of N_2 and argon measured in our experiment. It should be clear that the phase difference in Figure 5 is only defined up to an arbitrary constant. Under the assumption that the harmonic phases of both media do not differ where the corresponding harmonic emission times coincide, we have set the phase reference at harmonic 17. From the smooth progression of the phase difference between harmonic 15 and 21 it becomes obvious that this choice is not critical. At the same time, the beginning of this range of very similar phases is in agreement with the onset of the strong field approximation at harmonic 15. This measurement therefore demonstrates that the continuum dynamics of the EWP are very similar in both media.

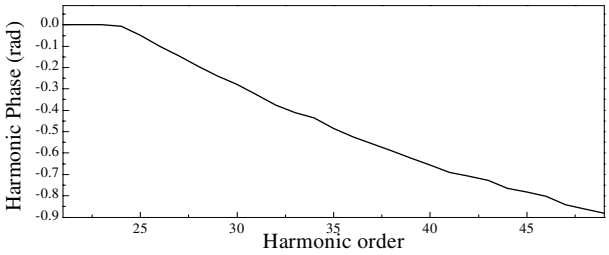

Fig. 6. Variation of the harmonic phases due to interference effects in N_2. Calculation for random alignment of the molecules, assuming the π-jump to start at harmonic order 25. For more details see text.

At high photon energy (harmonic 23 in Fig. 5) the congruence between the atomic and the molecular system seems to weaken again. One might wonder if this is not the onset of the π jump in the phase, due to the interference process in the recombination. However, in our experiment there is a random alignment of the N_2 molecules, so that we can expect some sort of smearing effect because when the alignment angle increases, the phase jump is shifted to a higher order. Using the two-center interference model, we can estimate the influence of random alignment on the resulting phase, as a function of the harmonic order. At a given orientation θ of the molecule there is a minimum in the harmonic amplitudes, at the order $q_m(\theta) = \pi h/4\omega_0 m_e r_0^2 \cos^2\theta$. We assume that the harmonic phase is flat, except for a π jump through the interference minimum: $\varphi_q = 0$ if $q < q_m(\theta)$ and $\varphi_q = -\pi$ if $q > q_m(\theta)$. We choose the distance r_0 between the two interference centres in nitrogen to be 0.1 nm, which corresponds to a minimum around harmonic 25 at $\theta = 0°$ as was measured in [11].

The resulting electric field $\mathfrak{E}_q$ composed of all contributions corresponding to different angles θ with respect to the laser polarisation is [30]

$$\mathfrak{E}_q \propto \int_{\theta=0}^{\pi/2} a_q(\theta) e^{-i(\varphi_q(\theta))} \sin(\theta) d\theta \tag{3}$$

where $a_q(\theta)$ and $\varphi_q(\theta)$ are the different harmonic efficiencies and phases for different angles. We assume here that the harmonic amplitudes do not vary with the angle. Figure 6 presents the phase of the resulting electric field as a function of the harmonic order. A phase variation is visible, but it is smoothed over harmonic orders $q > q_m(\theta = 0°)$. Furthermore, the magnitude of the jump is smaller than π.

As simple as this model is, we can draw some conclusions from the result: (i) a signature of the interference process is present in the harmonic phases, even with random alignment, and should therefore be measurable. Please note that the phase variation is even more pronounced if the decrease of the harmonic amplitude with increasing angle is taken into account. (ii) The magnitude of the phase variation is strongly affected by the averaging, making quantitative comparison with theory difficult. (iii) The jump starts at order 25, whereas in our measurements, we observe a deviation already at harmonic 23. Measurement of the phase of higher orders was prevented by the low photoionisation cross section of the detecting gas (argon) at these high photon energies.

In a very recent theoretical publication [31], the authors conclude that the admixture of both s and p atomic orbitals to the N_2 $3\sigma_g$ molecular orbital hampers an explanation of the interference pattern in the two-centre interference model. Therefore it is quite possible that the phase difference in our measurements reveals experimentally the complexity of the recombination process in N_2.

4 Perspectives

The measurement of the relative harmonic phases has important consequences on applications such as tomographic imaging of molecular orbitals [11]. Likewise it can offer a thorough comparison of theory and experiment for more complex molecules than H_2 [31].

In [11] Itatani et al. demonstrate the tomographic reconstruction of the N_2 $3\sigma_g$ orbital. To this end they generate harmonics in an ensemble of aligned N_2 molecules and measure the harmonic yield (17th to 43th) for 19 different angles θ. The harmonic spectrum can be considered as an experimental evaluation of the complex electric dipole $\mathfrak{D}$:

$$\mathfrak{D}(\omega) = \mathfrak{a}\left(k(\omega)\right) \int \Psi_g^*(\boldsymbol{r}) e \boldsymbol{r} e^{ik(\omega)x} d\boldsymbol{r}. \tag{4}$$

Here the recolliding electron wavepacket is expanded in a superposition of plane waves $\Psi_c = \int \mathfrak{a}(k) e^{ikx} dk$ with the complex amplitudes $\mathfrak{a}(k)$ while the harmonic frequency is ω.

Itatani et al. succeed in evaluating the integral in equation (4) (which in turn means determining the spatial Fourier components of $\boldsymbol{r}\Psi_g$) by applying a few assumptions which we will highlight in the following. A detailed expression of the complex harmonic spectrum for generation in N_2 and Ar is

$$|\mathfrak{S}^{N_2}(\omega)| e^{i\varphi^{N_2}} = \omega^2 |\mathfrak{a}^{N_2}\left(k(\omega)\right)| e^{i\varphi_c^{N_2}} \langle \Psi_g^{N_2} | e\boldsymbol{r} | e^{ik(\omega)x} \rangle \tag{5}$$

and

$$|\mathfrak{S}^{Ar}(\omega)| e^{i\varphi^{Ar}} = \omega^2 |\mathfrak{a}^{Ar}\left(k(\omega)\right)| e^{i\varphi_c^{Ar}} \langle \Psi_g^{Ar} | e\boldsymbol{r} | e^{ik(\omega)x} \rangle. \tag{6}$$

On the left hand side in both equations the complex spectrum is splitted in modulus (square root of the measured harmonic power spectrum) and phase. We note that $e^{i\varphi^{N_2}}$ and $e^{i\varphi^{Ar}}$ represent the total phase information, including the ionisation and continuum dynamics and the recombination of the EWP. On the right hand side the complex amplitudes $\mathfrak{a}(k)$ are also splitted in modulus and phase, where $e^{i\varphi_c^{N_2}}$ and $e^{i\varphi_c^{Ar}}$ include only the ionisation and continuum dynamics.

The authors in [11] now argue that the processes included in the first (ionisation) and the second step (continuum dynamics) are mainly identical in both media, N_2 and argon. Therefore they assume $\mathfrak{a}^{N_2}\left(k(\omega)\right) = \mathfrak{a}^{Ar}\left(k(\omega)\right)$.

Initially, we equate only the absolute value of these amplitudes, combine equations (5) and (6) and obtain

$$\left\langle \Psi_g^{\mathrm{N_2}} | e\boldsymbol{r} | e^{ik(\omega)x} \right\rangle = \left\langle \Psi_g^{\mathrm{Ar}} | e\boldsymbol{r} | e^{ik(\omega)x} \right\rangle \frac{|\mathfrak{S}^{\mathrm{N_2}}(\omega)|}{|\mathfrak{S}^{\mathrm{Ar}}(\omega)|} \times e^{i\left(\varphi^{\mathrm{N_2}} - \varphi^{\mathrm{Ar}}\right)} e^{-i\left(\varphi_c^{\mathrm{N_2}} - \varphi_c^{\mathrm{Ar}}\right)}. \quad (7)$$

The first term on the right hand side of equation (7) can be calculated, because the groundstate wavefunction in argon ($3p_x$) is known. The second term includes the measured harmonic spectra, i.e. is also known. Finally, the phase term shows that only the phase difference between N_2 and argon *in the recombination process* matters for the reconstruction. Following the interference model, the authors in [11] assume a π-jump in the harmonic phases of N_2 compared to argon where the harmonic yield goes through a minimum, in this case the 25th harmonic. With these two assumptions, the authors use the projection of the wavefunction for 19 different alignment angles to reconstruct the N_2 $3\sigma_g$ orbital by tomographic means.

It is clear that the measurement of the harmonic phases is necessary for an accurate tomographic imaging. Our data in Figure 5 on the total phase difference between (randomly-aligned) N_2 and argon already gives interesting information in view of such reconstruction. The similarity observed for the plateau harmonics indicates that the continuum electron dynamics (as well as the recombination dynamics) in both media resemble each other very much in the region investigated here, and thus partially validates the hypothesis done in [11].

The phase difference for the low harmonics 11/13 would indicate that, for these orders, the specific structure of the molecular Coulomb potential has to be taken into account in the ionisation and continuum step. The calibration with an 'atomic partner' thus becomes questionable. As a result, we think that in general low harmonics (approximately up to the 13th) should not be included in tomographic methods, even though the magnitude of the deviation is weak in the present case.

The phase difference for the 23rd harmonic indicates a complex recombination process, which in turn could influence the reconstruction of the molecular orbital. Also, the existence of the π-jump has not been experimentally confirmed so far.

To address this problem, we are currently preparing a follow-up experiment, in which we will align N_2 and measure the harmonic phases at different angles. Aligning the molecules should reveal the position and the shape of the π-jump. Measurements of intensities, phases and polarisation of the harmonics will be very valuable for theoretical modelling of the tomographic method applied to molecules of realistic complexity.

In conclusion, for the first time the high order harmonics generated in randomly aligned N_2-molecules have been spectrally characterised both in amplitude and phase. We have reconstructed the temporal profile of the attosecond pulses comprising the 11th–23rd harmonics. The main result is that atomic and molecular system reveal a strong similarity in pulse duration, timing with respect to the laser electric field and chirping (positive) under the same experimental conditions. This is a remarkable feature of strong field phenomena. A comparison of experiment and theory underlines the strong similarity. To complete the discussion we propose that subtle differences in the harmonic emission times and harmonic phases at low orders result from the different Coulombic potential of N_2, which influences the continuum dynamics of the EWP. At high order, the difference cannot be directly explained by the straightforward interference model, but indicates a more complex recombination process in N_2, that may be due to admixtures of s- and p-atomic orbitals to the N_2 $3\sigma_g$ orbital. The results show that the measurement of the harmonic phases in aligned N_2-molecules will help to clarify, in what way these differences will affect applications like tomographic reconstruction of molecular orbitals. They can also serve as a starting point for the theoretical modelling of more complex molecules.

We want to thank Jean Francois Herrgöttlein, Michel Perdrix, David Garzella and Olivier Gobert for their excellent work in providing the LUCA laser facility. For very valuable discussions we thank Manfred Lein, Jérome Levesque and Fabien Quéré. K.V. is on leave from the Department of Optics and Quantum Electronics, University of Szeged, Hungary. This research was supported by the Marie Curie European Program (MRTN-CT-2003-505138,XTRA and MEIF-CT-2004-009268), the Integrated Infrastructure Initiative (RII3-CT-2003-506350, LASERLAB-EUROPE), the Swedish Science Council and the Engineering and Physical Sciences Research Council of the UK.

References

1. A. McPherson, G. Gibson, H. Jara, U. Johann, T.S. Luk, I. McIntyre, K. Boyer, C.K. Rhodes, J. Opt. Soc. Am. B **4**, 595 (1987)
2. M. Ferray, A. L'Huillier, X.F. Li, L.A. Lompré, G. Mainfray, C. Manus, J. Phys. B **21**, L31 (1988)
3. M. Hentschel, R. Kienberger, Ch. Spielmann, G.A. Reider, N. Milosevic, T. Brabec, P. Corkum, U. Heinzmann, M. Drescher, F. Krausz, Nature **414**, 509 (2001)
4. R. Kienberger, E. Goulielmakis, M. Uiberacker, A. Baltuska, V. Yakovlev, F. Bammer, A. Scrinzi, Th. Westerwalbesloh, U. Kleineberg, U. Heinzmann, M. Drescher, F. Krausz, Nature **427**, 817 (2004)
5. P.M. Paul, E.S. Toma, P. Breger, G. Mullot, F. Augè, Ph. Balcou, H.G. Muller, P. Agostini, Science **292**, 1689 (2001)
6. Y. Mairesse et al., Science **302**, 1540 (2003)
7. P. Tzallas, D. Charalambidis, N.A. Papadogiannis, K. Witte, G.D. Tsakiris, Nature **426**, 267 (2003)
8. M. Drescher et al., Nature **419**, 803 (2002)
9. P. Johnsson, R. Lopez-Martens, S. Kazamias, J. Mauritsson, C. Valentin, T. Remetter, K. Varju, M.B. Gaarde, Y. Mairesse, H. Wabnitz, P. Salières, Ph. Balcou, K.J. Schafer, A. L'Huillier, Phys. Rev. Lett. **95**, 013001 (2005)
10. K. Varju, Y. Mairesse, B. Carré, M.B. Gaarde, P. Johnsson, S. Kazamias, R. Lopez-Martens, J. Mauritsson, K.J. Schafer, P. Balcou, A. L'Huillier, P. Salières, J. Mod. Opt. **52**, 379 (2005)

11. J. Itatani, J. Levesque, H. Niikura, H. Pépin, J.C Kieffer, P.B. Corkum, D.M. Villeneuve, Nature **432**, 867 (2004)
12. H.G. Muller, Appl. Phys. B **74**, S17 (2002)
13. Y. Mairesse, A. de Bohan, L.J. Frasinski, H. Merdji, L.C. Dinu, P. Monchicourt, P. Breger, M. Kovacev, T. Auguste, B. Carre, H.G. Muller, P. Agostini, P. Salieres, Phys. Rev. Lett. **93**, 163901 (2004)
14. P. Antoine, A. L'Huillier, M. Lewenstein, Phys. Rev. Lett. **77**, 1234 (1996)
15. M.B. Gaarde, K.L. Schaefer, Phys. Rev. Lett: **89**, 213901 (2002)
16. P. Kruit, F.H. Read, J. Phys. E Sci. Instrum. **16**, 313 (1983)
17. V. Veniard, R. Taieb, A. Maquet, Phys. Rev. A **54**, 721 (1996)
18. L.C. Dinu et al., Phys. Rev. Lett. **91**, 063901 (2003)
19. Y. Liang, A. Augst, S.L. Chin, Y. Beaudoin, M. Chaker, J. Phys. B **27**, 5119 (1994)
20. C. Lyngå, A. L'Huillier, C.G. Wahlström, J. Phys. B. **29**, 3293 (1996)
21. R. Lopez-Martens, K. Varju, P. Johnsson, J. Mauritsson, Y. Mairesse, P. Salieres, M.B. Gaarde, K.J. Schafer, A. Persson, S. Svanberg, C.-G. Wahlstrom, A. L'Huillier, Phys. Rev. Lett. **94**, 033001 (2005)
22. S. Kazamias, Ph. Balcou, Phys. Rev. A **69**, 063416 (2004)
23. P. Corkum. Phys. Rev. Lett. **71**, 1994 (1993)
24. K.C. Kulander, K.F. Schafer, J.L. Krause, In *Super-Intense Laser-Atom Physics* (NATO ASI B316, 1993), page 95
25. M. Lewenstein, Ph. Balcou, M. Yu. Ivanov, A. LHuillier, P.B. Corkum, Phys. Rev. A **49**, 2117 (1994)
26. T. Kanai, S. Minemoto, H. Sakai, Nature **435**, 470 (2005)
27. M. Lein, N. Hay, R. Velotta, J.P. Marangos, P.L. Knight, Phys. Rev. Lett. **88**, 183903 (2002)
28. M. Lein, N. Hay, R. Velotta, J.P. Marangos, P.L. Knight, Phys. Rev. A **66**, 023805 (2002)
29. C. Vozzi et al., Phys. Rev. Lett. **95**, 153902 (2005)
30. M. Lein, R. de Nalda, E. Heesel, N. Hay, E. Springate, R. Velotta, M. Castillejo, P.L. Knight, J.P. Marangos, J. Mod. Opt. **52**, 465 (2005)
31. B. Zimmermann, M. Lein, J.M. Rost, Phys. Rev. A **71**, 033401 (2005)